

**ELECTROPHYSICAL PROCESSES OF ELECTRON AVALANCHE DEVELOPMENT IN AIR
IN THE DEVICE OF PULSE DIELECTRIC BARRIER DISCHARGE****Yu.M. Vasetsky*****Institute of Electrodynamics National Academy of Sciences of Ukraine,
Beresteisky Ave., 56, Kyiv, 03057, Ukraine.****E-mail: yuriy.vasetsky@gmail.com.**

The purpose of the work is to study the influence of the size of the discharge gap and the time dependence of the increase in the pulsed electric field to the characteristics of the avalanche stage of a pulse dielectric barrier discharge (PDBD) from the beginning of electron drift in increasing electric field, taking into account the threshold nature of the impact ionization process in the gas, the influence of photo-ionization to the enlargement of avalanches, diffusion and electrostatic repulsion of electrons at the head of the avalanche. Computational studies were carried out for the specific electrode system with the dielectric barrier located on the cathode for gas gaps 1–3 mm, voltage pulse with the amplitude of 25 kV and time of its achievement of 50 ns. It is established that after three or four stages, the electric field strength of the avalanche-streamer transition has a value of 80–100 kV/cm, which occurs ~30 ns after the voltage is applied, and weakly depends on the size of the gas gap. For the test experiment with gap of 1.5 mm, such values occur at the moment of reaching the maximum current value. It is determined that the size of the electron avalanche for the given voltage pulse in the PDBD is determined by the process of electron diffusion. It is shown that after applying voltage as a result of the first stage of electron drift, the number of emitted photons capable of generating effective electrons for the further development of the avalanche process strongly depends on the size of the discharge gap. The limits of the discharge gaps with significantly different possibilities to initiate the avalanches at subsequent stages are determined. References 22, figures 9, tables 2.

Key words: pulse dielectric barrier discharge, avalanche-streamer transition, photo-ionization, electric field strength of electron avalanche.

Introduction. Among the numerous applications of electric discharge in gas, studies of the PDBD have become relevant in recent years [1–3]. The qualities of this type of discharge have proven useful in technologies that require sufficiently energetic electrons and their homogeneous distribution with a significant density in the discharge gap. For this purpose, the pulsed electric field with a significant overvoltage is used, which during tens nanoseconds reaches its maximum value in discharge gaps of the millimeter range. Overvoltage in experiments can reach 50% and even 100% and more. Homogeneity of the discharge in the form of electron avalanches and streamers without the formation of separate spark channels is realized when using a dielectric barrier in the form of dielectric plates covering one or both electrodes.

From the point of view of efficiency for technological purposes, pulse barrier discharge is an alternative to other types of discharges used for the same purpose [4]. In particular, it was shown that it is appropriate to introduce devices based on this type of discharge for the generation of ozone and other active radicals in the technologies of processing food products, contaminated water and air [5–7]. Another possible direction is the treatment of metal surfaces with high-energy electrons generated in the discharge to improve the mechanical properties of the surface layer [8, 9].

Successes in experimental research of the PDBD are to a lesser extent supported by theoretical substantiation of the features of electrophysical processes, which is expedient for determining directions of improvement of its characteristics. The complex and multifaceted nature of electrophysical processes in electric

© Vasetsky Yu.M., 2025

* ORCID: <https://orcid.org/0000-0002-4738-9872>

© Publisher PH “Akadempriodyka” of the National Academy of Sciences of Ukraine, 2025



This is an Open Access article under the CC BY-NC-ND 4.0 license
<https://creativecommons.org/licenses/by-nc-nd/4.0/legalcode.en>

discharge in general and to no less extent in PDBD determines the priority of the experimental direction of work. However, this does not exclude also theoretical research, which goes in parallel with the experiment. In this regard, we note a colossal number of journal publications and a large, but much smaller number of monographic literature. According to the well-known gas discharge researcher Y. Reiser, when it comes to theory, this is not least due to the extremely complex, multifaceted and confusing effects [10]. Therefore, since this article is primarily aimed to obtain an idea of electrophysical processes, references are limited mainly to several literary sources, which provide a sufficient amount of the necessary original literature. These are primarily books that contain information about gas discharges of various types and directly about pulsed discharges [10–16]. For the same reason, the study in the article is limited only to a certain initial stage of the development of a pulsed barrier discharge, which, however, allows us to get an idea not only about the dynamics and characteristics of this stage, but also to obtain practically necessary information.

A feature of the work is the study of a specific electrode system, to which a voltage pulse with a given amplitude and time dependence is applied. Such restrictions correspond to typical values of the parameters of an experimental device that is being developed for the possibility of technological use [17, 18]. In addition, this allows us to limit the scope of the paper and provide an overview of a significant amount of relevant data and performance characteristics of this device. The study of the specific system can simultaneously indicate approaches for a more general study of the PDBD.

The aim of the work is to determine the influence of the size of air gap and the time dependence of the increase in the pulsed electric field to the characteristics of the avalanche stage of the PDBD from the beginning of electron drift in the increasing electric field, taking into account the threshold nature of the impact ionization process in the gas, the influence of photo-ionization to increase in the number of avalanches, diffusion and electrostatic repulsion of electrons until the moment when the conditions for the beginning of the streamer process are reached at the avalanche head.

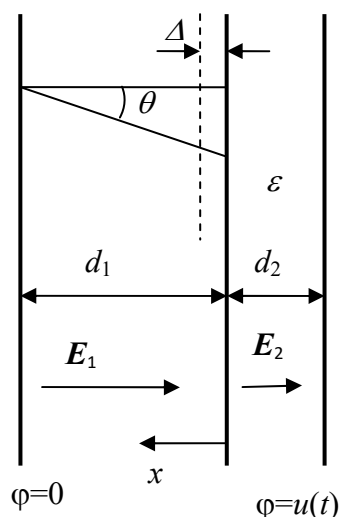


Fig. 1

Problem statement. It is considered the formation of an electric discharge in a flat system of electrodes to which the voltage pulse $u(t)$ is applied. On the surface of the negative polarity electrode (cathode) there is a dielectric barrier in the form of a flat dielectric plate of thickness d_2 with relative dielectric permittivity ε . The discharge is formed in air gap of thickness d_1 at atmospheric pressure $p = 10^5$ Pa (Fig. 1).

The PDBD in the electric discharge installation. Fig. 2, a shows a typical form of the dependences for a single voltage pulse (red curve 1) and current (blue curve 2) in experiments with the PDBD in a system of flat electrodes, to which pulses are applied, repeating at a frequency of 100 Hz [17, 18]. The negative values of voltage and current correspond to the designations of the potentials in Fig. 1 and the choice of the positive direction of the current along the axis x . The presented oscillograms were obtained for electrodes with a diameter of 28 mm and distance $d_1 = 1.5$ mm, the dielectric barrier with thickness of $d_2 = 1$ mm had a relative dielectric permittivity $\varepsilon = 4.74$. The voltage at the initial stage increases very gradually, its change becomes noticeable only starting from the time point $\sim 10\text{--}20$ ns from the beginning of the presented dependences. Without taking into account the almost zero initial stage, the pulse duration until reaching the maximum value is approximately $t_m = 40\text{--}50$ ns. The measurement results in the experimental technological device, where another electrode system is implemented [7], are shown in Fig. 2, b. Here the same characteristic features are observed, in particular, the current reaches its maximum value in modulus at the voltage before it reaches its amplitude value. Here the same characteristic features are observed, in particular, the current reaches its maximum value in modulus at the voltage even before it reaches its amplitude value. A certain difference consists in the existence of an additional local extremum on the decreasing modulus section of the current curve after its maximum value. This circumstance may be due to the nature of the electrophysical processes in the pulsed barrier discharge, and it will be discussed at the end of the article.

In the mathematical model for studying pulsed barrier discharge in the uniform electric field (Fig. 1), the intensity of the external electric field in the gas gap $E_1 = E_0$ (without taking into account the parameters associated with the electric discharge: volume and surface charges, charge transfer current, etc.) is defined as

$$E_0(t) = \frac{u(t)}{d_1 + d_2/\varepsilon}. \quad (1)$$

The maximum value of the pulsed field strength in the example presented in Fig. 2, *a* is equal to $E_{0\max} \approx 130 \cdot 10^5$ V/m. In comparison, the breakdown voltage for the same air gap in a constant field has a much smaller value $\approx 43 \cdot 10^5$ V/m. The corresponding data based on the results of various authors are given in [11] and shown in Fig. 3. It is significant that the pulsed discharge, depending on the rate of voltage increase and the distance between the electrodes, can occur at a much higher voltage compared to the constant voltage [12].

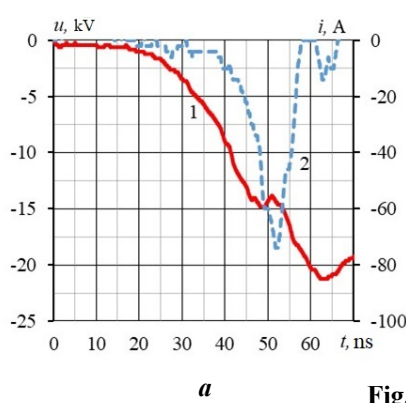
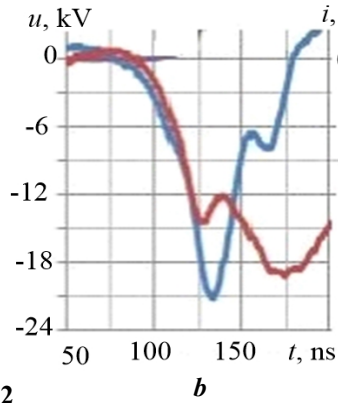


Fig. 2



b

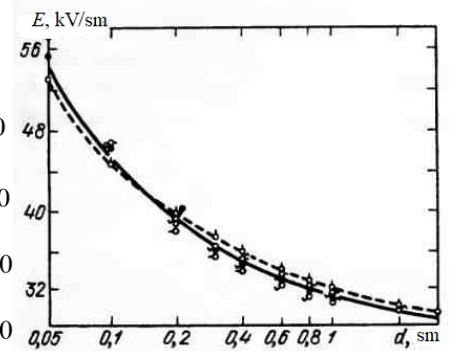


Fig. 3

The current in the discharge gap begins to increase sharply at approximately the same electric field strength as the electric discharge in constant field. The current in this case increases to a maximum value during ~ 10 ns and reaches it at the external field strength of $E_0 \sim 90 \cdot 10^5$ V/m. Then the current decreases and, after a slight surge, takes on a zero value approximately at the time of reaching the maximum voltage value, which is characteristic of the capacitive component of the current. Visually, photographs and high-speed videos show that a homogeneous discharge can be in the form of a homogeneous glow or consist of a significant number of individual luminous filaments [6].

The electric discharge process in the presence of the dielectric barrier cannot end with an electric discharge in the classical sense, in particular: the Townsend mechanism of a pulsed discharge at such significant overvoltage is unlikely [12]; the development of a single spark channel contradicts experimental data, its development is prevented by the presence of a dielectric barrier. On the other hand, the ignition of a discharge at a significant overvoltage may indicate the possibility of the formation of streamers, but as a multi-channel process. Such features necessitate research of the pulsed discharge process in the presence of the dielectric barrier at the cathode, taking into account the specific conditions for applying voltage to the electrode system.

The pulsed electric discharge process, including its avalanche stage, is a multifaceted phenomenon, which includes, in particular, the process of increasing their number as a result of ionization phenomena, electron diffusion, radiation and photo-ionization, excitation of neutral molecules, creation of a volume charge along the entire path of the avalanche, including the special importance of the maximum field of the avalanche head, and many others. In this work, the electric discharge process is analyzed based on the consideration of the development of one avalanche of electrons. Thus, it is assumed that the field strength of the volume charge of all avalanches, including the positive charge of the ion trace, is insignificant compared to the field of the external field of the source. Such consideration makes it possible to focus on the main factor in this case - the achievement of the local field near the avalanche head to the value at which the streamer phase of the process begins.

Processes at the initial stage of applying pulsed voltage. The development of avalanche begins with an initial electron, which, multiplying, turns into electron avalanche drifting in increasing field. The voltage at the initial stage, based on Fig. 2, for estimates we will describe by the power function $u(t) = k(t - t_b)^n$. The value of $t_b \sim (10 - 20) \cdot 10^{-9}$ s can be taken as the beginning of the dependence. The parameter $k(n)$ depends on the degree of the chosen approximation. At $n = 2$ this parameter for the given example is equal

approximately $k \approx 2 \cdot 10^{19} \text{ V/s}^2$. The drift velocity of electrons in the electric field $v_{ed} = \mu_e E$ is proportional to its mobility μ_e . The mobility value for air at atmospheric pressure is assumed to be independent of the electric field strength $\mu_e \approx 5 \cdot 10^{-2} \text{ m}^2/(\text{V} \cdot \text{s})$ [13]. Then, taking into account (1), the time point $t - t_b$ and the electric field strength E , when the electron has moved a distance $x - x_0$ from the initial point x_0 from the start moment of voltage application, are as follows

$$t_1 - t_b = \left[\frac{(x - x_0)(n+1)(d_1 + d_2/\varepsilon)}{\mu_e k} \right]^{1/(n+1)}. \quad (2)$$

$$E_0(x - x_0) = \left[\frac{(x - x_0)(n+1)}{\mu_e} \right]^{n/(n+1)} \left(\frac{k}{d_1 + d_2/\varepsilon} \right)^{1/(n+1)}. \quad (3)$$

The greatest field strength will be obtained in the case $x - x_0 = d_1$, that is, for an electron that has moved the maximum distance from the dielectric barrier to the opposite electrode. Table 1 shows the maximum electric field strengths E_0 and times $t - t_b$ at the end of the electron motion for different air gaps d_1 at the same voltage value and its dependence on time. Here and in the following we will consider distances in a limited range of values that are more often used in experiments $d_1 = 1 \div 3 \text{ mm}$. Other parameters of the electrode system are left the same as in the experiment, the results of which are shown in Fig. 2, *a*.

Table 1

$d_1, \text{ mm}$	$E, 10^5 \text{ V/m}$	$t - t_b 10^{-9}, \text{ s}$
1.0	39	15
1.5	46	19
2.0	51	24
3.0	59	32

From the data in Table 1 it is clear that at the considered initial stage for small distances the field strength does not reach the values of the electric breakdown. Even for larger distances the strength is still much lower, compared to the field strength, where the current in Fig. 2, *a* reaches a maximum, which indicates a change in the processes in the development of the electric discharge. In addition, when considering the initial stage of the development of the electric discharge phenomenon, it is necessary to take into account the different nature of the dependences on the field strength of the electron drift and the ionization of neutral molecules. The latter, unlike the electron drift, has a threshold nature - ionization occurs only from a certain threshold value of the electric field strength. This value for electronegative gases is determined by the strength when the ionization coefficient begins to exceed the attachment coefficient. For air, the ratio of the field strength to the gas pressure, these coefficients are equal at $E/p \approx (26 - 31) \text{ V}/(\text{m} \cdot \text{Pa})$ [19]. This explains the significant importance of the rate of voltage increase, especially at the initial stage, since here the voltage usually increases over time not linearly, but rather according to a law close to quadratic.

Parameters included in the calculation of processes in the PDBD. Since for calculations it is necessary to take into account the change in voltage at least until the maximum value, we will use an approximation in the form in which for small values of time the dependence repeats the already applied approximation

$$u(t) = U_m \sin^n(\omega t). \quad (4)$$

As an example, Fig. 4, *a* shows the dependences of the change in the electric field strength over time for a number of air gap values d_1 when applying voltage with the amplitude $U_m = -25 \cdot 10^3 \text{ V}$ at $n = 2$, $\omega = \pi \cdot 10^7 \text{ s}^{-1}$, which corresponds to the time of reaching the maximum value $t_m = 50 \cdot 10^{-9} \text{ s}$. The rate of voltage change $\frac{du(t)}{dt} = \omega U_m \sin(2\omega t)$ reaches at $t = \pi/(4\omega)$ the maximum value $\omega U_m = 0.8 \cdot 10^{12} \text{ V/s}$ which is close to the values used in the developed pulsed power sources [17] and in experiments [6].

Starting from the threshold value, the ionization coefficient (number of ionizations when an electron moves over distance 1 m under the action of electric field) increases. For quantitative analysis, we will use the most common approximation of experimental data in the form [12]

$$\frac{\alpha}{p} = A \exp\left(-\frac{B}{E/p}\right), \quad (5)$$

where the coefficients A and B differ slightly from different authors [10, 12, 14, 20]. For further calculations, the following values [20] in the SI system of units, valid for discharges in air, are used:

$$\begin{aligned} E/p = 15 - 114 \text{ V/(m} \cdot \text{Pa)}: \quad A_1 = 6.46 \text{ 1/(m} \cdot \text{Pa)}, \quad B_1 = 190 \text{ V/(m} \cdot \text{Pa)}; \\ E/p = 114 - 460 \text{ V/(m} \cdot \text{Pa)}: \quad A_2 = 11.1 \text{ 1/(m} \cdot \text{Pa)}, \quad B_2 = 277.4 \text{ V/(m} \cdot \text{Pa)}. \end{aligned} \quad (6)$$

In (5) and (6) the data refer to the effective ionization coefficient, which is the difference between the actual ionization coefficient and the attachment coefficient.

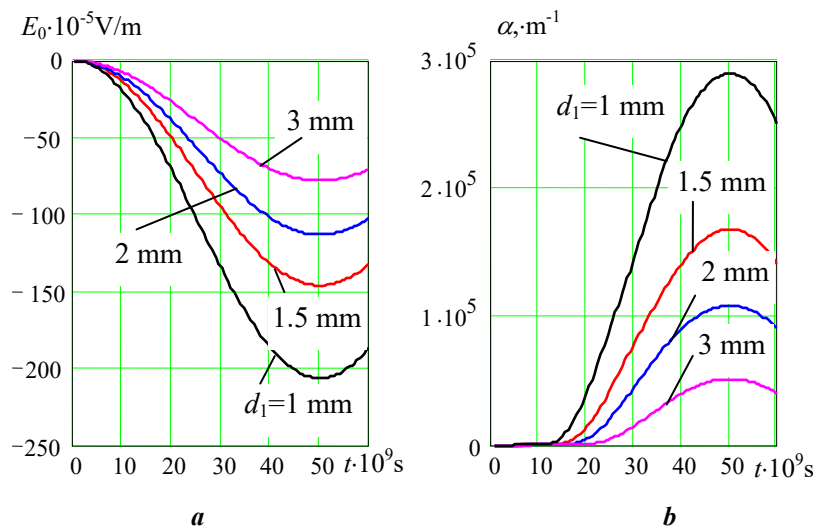


Fig. 4

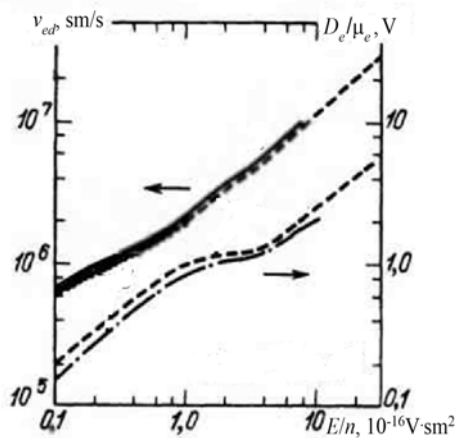


Fig. 5

Since the electric field strength changes in time, the ionization coefficient $\alpha(E(t))$ changes accordingly. Fig. 4, b shows the dependences of the ionization coefficient on time for the selected voltage pulse and different air gaps. The values of the coefficients A and B are adjusted to each other in different ranges of the ratio E/p . From the comparison of the data in Fig. 4, b and Table 1, it follows that for the initial stage of applying voltage pulse during the movement of the electron avalanche over the distance d_1 , the value of the ionization coefficient α is still far from the maximum magnitude that can be achieved for this interval. Therefore, the electric discharge process can develop further by increasing the number of electrons in the avalanche or new avalanches due to the mechanisms of the appearance of initial electrons at a later time.

In each electron avalanche, during its movement in the electric field and the growth of the number of electrons, the process of their diffusion takes place. This process develops simultaneously with the electrostatic repulsion of electrons in the avalanche. These processes affect the size of the avalanche and it, together with the number of electrons in the avalanche, directly determines the electric field of the volume charge, which is added to the field of the external source. The transition of the avalanche form of the discharge to the streamer form occurs when the electric field strength created by the volume charge E' of electrons reaches approximately the magnitude of the external field

$$|E'| \approx |E_0|, \quad (7)$$

This condition or the associated critical number of electrons in an avalanche $N_e = 10^6 - 10^8$ are given in the results of many studies [10–12, 15]. In the following, in contrast to the current value, the field strength under condition (7) will be denoted as E_s .

The parameters necessary for studying the discharge development process based on condition (7), namely the electron diffusion coefficient D_e , their mobility μ_e , and the electron temperature T_e , which can differ significantly from the gas temperature, depend on the electric field strength, which for the pulsed mode varies in time. These quantities are not independent and are related by Einstein's general thermodynamic relation

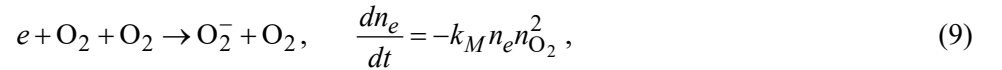
$$\frac{D_e}{\mu_e} = \frac{kT_e}{e}, \quad (8)$$

where k is the Boltzmann constant, e is the electron charge.

For further analysis, data from [10] are used, which are presented in Fig. 5 in graphical form. The calculated (dashed curves) and experimental (solid curves) results for the drift velocity $v_{ed} = \mu_e E$ and characteristic energy D_e/μ_e are given as a function of the ratio of the electric field strength to the number of molecules per unit volume E/n .

Mechanisms of the appearance of initial electrons in the electrode system of pulsed barrier discharge. The estimated movement of the electron avalanche and, accordingly, the electric field strength (2), (3) assumed the existence of initial electrons. Since at the initial stage from the moment of applying the voltage pulse, at least for $d_1 \leq 1.5$ mm, the conditions for the transition of the avalanche discharge into a streamer discharge are not yet created, then for the continuation of the ionization process there must be a mechanism for restoring the initial electrons, which move already at a higher pulse voltage. What is this mechanism is not investigated in this work; however, it is assumed that such electrons appear due to certain mechanisms, in particular, detachment from negative ions and photo-ionization.

If we consider a single pulse or the first of a sequence of pulses, then the initial electrons in the initial period are those that appeared due to the natural background radiation. Under the influence of such radiation, the rate of appearance of electrons in the air is $dn_e/dt = 10^6 - 10^7 \text{ m}^{-3} \cdot \text{s}^{-1}$ [12], where n_e is the electron density. The presence of oxygen in the air leads to the attachment of electrons. This process in dry air occurs most effectively in triple collisions, which is described by equation [10]



where the experimental value of the reaction rate constant is $k_M = 2.5 \cdot 10^{-42} \text{ m}^6/\text{s}$. Hence, the electron density decreases in time from the initial value n_{e0} according to exponential law with the time constant τ_M

$$n_e = n_{e0} \exp(-t/\tau_M), \quad \tau_M = 1/(k_M n_{O_2}^2), \quad (10)$$

which is found to be $\tau_M = 12.5 \cdot 10^{-9} \text{ s}$. It differs slightly from the value $\tau_M = 11 \cdot 10^{-9} \text{ s}$, which takes into account the intermediate excited states of oxygen molecules [10]. The result obtained implies that almost all electrons that appear as a result of natural ionization very quickly attach to oxygen molecules, the ions of which can no longer create avalanche of electrons in the electric field.

In the strong electric field, the attachment rate increases with increasing field strength, and the faster the higher the air humidity [19].

The dynamics of the appearance of electrons as a result of detachment from oxygen ions is also described by the exponential law of the decrease in the density of negative ions from the initial value $n_{0 O_2^-}$.

The time constant τ_d characterizes the “lifetime” of negative ions and is determined by the constant rate of electron detachment $k_d = 10^{-20} \text{ m}^3/\text{s}$ [10]

$$n_{O_2^-} = n_{0 O_2^-} \exp(-t/\tau_d), \quad \tau_d = 1/(k_d n_L), \quad (11)$$

where n_L is the density of gas molecules, which for normal conditions of the air under consideration is the Loschmidt number $n_L = 2.69 \cdot 10^{25} \text{ m}^{-3}$. From (11) we obtain the time constant $\tau_d = 3.7 \cdot 10^{-6} \text{ s}$.

During the time the pulse reaches its maximum value t_m in the space between the dielectric barrier and the anode, electrons with the density $n_e = n_{0 O_2^-} [1 - \exp(-k_d n_L t_m)]$ may appear as a result of detachment.

For example, for the selected time $t_m = 50 \cdot 10^{-9} \text{ s}$, the value of the density of the detached electrons will be $n_e \approx n_{0 O_2^-} 1.3 \cdot 10^{-2} \text{ m}^{-3}$. If the density $n_{0 O_2^-}$ is determined by the process of natural ionization of the air

with subsequent attachment, then at $n_{0\text{O}_2^-} \sim 5 \cdot 10^8 \text{ m}^{-3}$ [13] we have $n_e \approx 7 \cdot 10^6 \text{ m}^{-3}$. In the volume of the air gap with the surface of the electrodes S , initial electrons $7 \cdot 10^6 S d_1$ will appear during considered time. In this case, in the experiment, the oscillograms for which are shown in Fig. 2, *a*, only ~ 10 electrons appears at an arbitrary point in space with equal probability in the time interval. These electrons in the electric field multiply and move towards the anode. The process of increasing the number of electrons is more effective, the closer to the barrier the initial electron appears and the greater the field strength at the moment of electron detachment. In addition, it is noted that in air in the electric field, the efficiency of electron detachment from negative ions O_2^- is maximum at $E/p = 68.5 \text{ V}/(\text{m} \cdot \text{Pa})$ [12].

Since in the device in which the electric discharge processes are analyzed, the pulses follow each other with a frequency of 100-200 Hz, the effective initial electron will appear, if not in the first, then in one of the nearest subsequent pulses. The described process may be more effective with a much higher density of negative ions, which will remain, for example, as a result of the previous pulse discharge. And indeed, in experiments, stabilization of the discharge is observed after a certain number of initial pulses.

It is believed that the initiation of avalanche processes may be associated with the phenomenon of photo-ionization. The ionization of molecules in an electron avalanche is a source of photons, which in their energy spectrum have a sufficient number of photons with energies capable of leading to the ionization of molecules. There are several ionization mechanisms involving photons, a detailed list of which is given in [10]. After the establishment by H. Raether [15] of the fact of gas ionization by a spark discharge, experiments were conducted on ionization by radiation from electron avalanches [21, 22]. In contrast to the spark discharge, an essential feature of the pulsed barrier discharge is its distribution over almost the entire area of the electrodes. This feature most likely is directly related to the initiation of a multichannel discharge by photons appearing in the heads of the electron avalanche and the streamer. Their number increases sharply both due to the exponential growth of the number of electrons in a single avalanche and the growth of the number of avalanches and streamers in the increasing pulsed field.

Let us give some estimates of the ionization by photons, which generate initial electrons in air. The impact ionization of molecules in the air is accompanied by the emission of photons of different frequencies. Such radiation is characterized by a set of parameters η_j , which is defined as the number of photons of a certain frequency per one ionizing of electron collision with neutral molecule. The values of η_j , for the frequencies at which the photo-ionization process is possible, are within $\eta_j = 10^{-3} \div 10^{-2}$, and their values also depend on the electric field strength [22]. The radiation intensity at the certain frequency directly at the head of the avalanche at zero distance from it $r = 0$ can be determined as the product $N_j(0) = N_e \eta_j$, where N_e is the number of electrons in the avalanche. For estimates, we will take the value $\eta_f \approx 5.4 \cdot 10^{-3}$ for the radiation of nitrogen molecules with a wavelength $\lambda = 101.2 \text{ nm}$ and the corresponding radiation intensity $N_f(0) = N_e \eta_f$.

The radiation in air with distance r from the source for each frequency is attenuated by the law $\exp(-k_j r)$, where the absorption coefficients k_j depend on the frequency of radiation. Their values according to measurements for air at atmospheric pressure are within $150 \div 2200 \text{ m}^{-1}$. As an average value for the characteristic field strength, we will take the value $k_f \approx 460 \text{ m}^{-1}$, which corresponds to the same length of the electromagnetic wave $\lambda = 101.2 \text{ nm}$. The characteristic distance at which the number of photons decreases by a factor of e , is $k_f^{-1} \approx 2 \cdot 10^{-3} \text{ m}$ and it is commensurate with the air gap d_1 . But this may be insignificant, considering that for the appearance of subsequent avalanches in growing pulsed electric field, a small number of initial electrons is sufficient, which can appear in a narrow gap near the barrier.

From the point of view of increasing the number of electrons in the avalanche reaching the anode, the most effective initial electrons generated by the photo-ionization are those that appear near the dielectric barrier in a layer of a certain thickness Δ , shown in the upper part of Fig. 1. The largest number of electrons in avalanche, in which the condition of transition into the streamer has not yet been reached, will be when it approaches the anode. Here, photons $N_f(0)$ are emitted from the avalanche head in all directions. Under the as-

sumption that the decrease in the intensity of the photon flux is associated with photo-ionization, we obtain the maximum possible value of the acts of appearance of initial electrons. In this case, it is easy to find the total number of photons within the thickness of the layer Δ , which lead to photo-ionization. The ratio of their number to the number of electrons in the avalanche N_{0f}/N_e is estimated from the following expression

$$\frac{N_{0f}}{N_e} = 2\pi\eta_f \int_0^{\theta_m} \left[\exp\left(-k_f \frac{d_1}{\cos\theta} \left(1 - \frac{\Delta}{d_1}\right)\right) - \exp\left(-k_f \frac{d_1}{\cos\theta}\right) \right] d\theta, \quad (12)$$

where $\theta_m = \arctg(D/d_1)$ is close to $\pi/2$, since the characteristic size of the electrodes D significantly exceeds the distance d_1 .

Relation (12) allows us to estimate the minimum number of electrons in avalanche near the anode, the radiation of which, due to photo-ionization, generates at least a few new initial electrons that will initiate new avalanches. So, within the limits $\Delta/d_1 = 0.1 \div 0.2$ for $d_1 = 1.5 \cdot 10^{-3}$ m the relation gives $N_{0f}/N_e = (1.7 \div 3.5) \cdot 10^{-3}$. Hence, for example, for ten new electron avalanches, it is necessary to have a maximum number of electrons in the head of the first avalanche not less than $N_e \geq (3 \div 6) \cdot 10^3$. For other sizes of the air gap, the corresponding number of electrons differs slightly in order of magnitude.

In the case when the number of electrons in the avalanche significantly exceeds the minimum value, expression (12) gives the number of new avalanches of the second generation stage caused by the previous avalanche of electrons. Since the intensity of the pulsed electric field is significantly higher in the second stage, the number of ionizations in the avalanches will also lead to larger number of emitted photons. This process can become quite intense even before the avalanche reaches the anode. Below is an analysis of the distance the avalanche overcomes and the number of electrons in it. Here we note that for the estimation of the number of photons from (12) it is necessary to choose a correspondingly smaller value $x_s < d_1$ instead d_1 and to expand the range of the region Δ where photoelectrons are generated. Moreover, the equation (12) can be used also, when the number of electrons approaches the critical value under the condition (7) of the avalanche-streamer transition in the middle of the gas gap. In this case, to obtain the estimate of the number of photons can be obtained from (12), where the distance x_s from the dielectric barrier to the coordinate of the avalanche head with the critical number of electrons can be accepted.

Since the main goal of the work is to study the development of avalanches until the conditions of the start of the streamer process, the processes of the appearance of initial electrons, the increase in the number of avalanches due to subsequent photo-ionization, and the multi-channel avalanche state are not considered in more detail. However, it is believed that the barrier discharge occurs under conditions when there is a sufficient number of initial electrons that generate the avalanche process.

Electron avalanches in the pulsed field of the barrier discharge device. A feature of the development of the avalanche process when the dielectric barrier is located at the cathode, in contrast to the free cathode, is that there is no emission of electrons from the cathode. As a result of electron detachment from negative ions or photo-ionization, electrons can appear at any point in the discharge space at any moment of the pulsed electric field action. For one individual avalanche the initial values of the time and coordinates of the electron appearance are denoted as t_0 and x_0 .

The electric field strength of avalanche charges distributed in the volume is insignificant throughout the entire time of avalanche growth, almost until the condition of transition into a streamer is reached [10]. Therefore, all parameters up to this point will be considered dependent on the external field strength in the air gap $E_0(t)$.

Taking into account the dependence of the parameters on the electric field strength, which varies in time, the distance that electrons move over time and the number of electrons in a single avalanche are determined by the following expressions

$$x(t) - x_0 = \int_{t_0}^t v_{ed}(t) dt, \quad (13)$$

$$N_e(t) = \exp \left(\int_{t_0}^t \alpha(t) v_{ed}(t) dt \right), \quad (14)$$

where the data in Fig. 5 are used for $v_{ed}(E(t))$, and for interpolation beyond the values of the electric field strength in the figure, the dependence $v_{ed}(E) \sim \sqrt{E}$ [10, 13] is used. The ionization coefficient is determined by approximation (5), (6). In expressions (13), (14) the time and movement of electrons are limited by the avalanche reaching the opposite electrode or its transition into streamer $x(t) - x_0 \leq d_1 - x_0$.

For the selected range of the air gap $d_1 = 1 - 3$ mm, the time required for the electrons to reach the anode due to drift in the pulsed electric field is significantly less than the time of the maximum field strength $t_m = 50$ ns. This can be seen from the time dependences on the coordinate x (Fig. 1) presented in Fig. 6. If the movement of electrons does not begin from the dielectric barrier, but at a distance from it, then on the corresponding curve it is necessary to choose a limited range of distances from zero to $x - x_0$.

Since the voltage and, accordingly, the field strength at the initial stage at $t_0 = 0$ increases gradually, the time for electrons to reach the anode significantly exceeds the values required to reach the anode at subsequent stages at higher pulse field strengths. At field strength approaching its maximum value, the time required to cross the entire gap for $d_1 = 1$ mm does not exceed 3 ns. This time increases for larger distances, but even for $d_1 = 3$ mm it is $t \sim 10$ ns, which is still significantly less than the time t_m to reach the maximum pulse voltage. The results presented allow us to compare the nature of the avalanche movement with their growth and the increase of the field strength distributed charge near the "heads" of the avalanches at different time intervals.

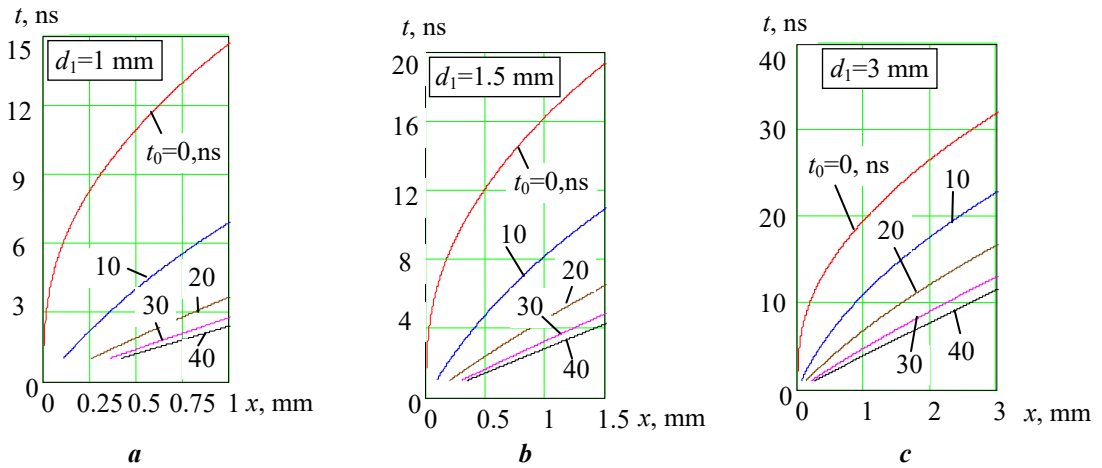


Fig. 6

The results of calculating the number of electrons in avalanche depending on the path moved by the avalanche from its origin at different initial times t_0 for different air gaps d_1 are shown in Fig. 7. Here, similarly to Fig. 6, in order to obtain data under the condition of the start of electron movement from the coordinate x_0 , it is necessary to limit the curves to the distance $x - x_0$, starting from the zero value.

Comparison of the curves at $t_0 = 0$ for different air gaps shows a significant dependence of the electric discharge processes at the initial stage on the size of the gap d_1 in the range under consideration. For $d_1 \leq 1.5$ mm the maximum number of electrons in the avalanche is probably insufficient for the appearance at least one ionizing photon. The minimum number of electrons in the avalanche turns out to be less than the value determined from (12), which is estimated by the value $N_e \sim 10^3 - 10^4$. For these gaps, at the first stage, all electrons that existed in the gap before the voltage was applied will move to the anode and there will be no necessary initial electrons left in the gap, for the appearance of which, as noted, a much longer time than ~ 15 ns (see Fig. 6, a). The mechanism of ignition of the pulsed discharge observed in experiments is not entirely clear and requires additional research. One possible mechanism may be a significant reduction

in the time of detachment of electrons from negative oxygen ions at a significantly higher intensity of the increasing pulsed field (Fig. 4, *a*).

For air gaps $d_1 > 1.5$ mm, after the first stage of the gap crossing by avalanche, the conditions of a multichannel avalanche process are fulfilled. In addition note for gaps $d_1 = 3$ mm (Fig. 7, *d*) and larger, the appearance of a number of electrons in the avalanche $N_e = 10^6 - 10^8$ sufficient to start the streamer process takes place already at the first stage after the voltage pulse is applied. This circumstance can lead to the localization of individual discharge channels, which is indeed observed in experiments for such gaps and also depends on the pulse repetition frequency [6].

The air gap $d_1 \sim 1.5$ mm seems to be intermediate from the point of view of the development of the pulsed barrier discharge. For this gap, only single photoelectrons probably appear at the first stage. But already at the second stage, starting from the time point ≈ 20 ns in a much stronger field, the number of electrons in the avalanche increases rapidly. Their number can reach the critical value necessary for the appearance of streamer, even in the central part of the gap. In this case, a significant number of photons $N_e \eta_f$ can lead to photo-ionization of the gas in larger volume than at the first stage of the development of the electron avalanche.

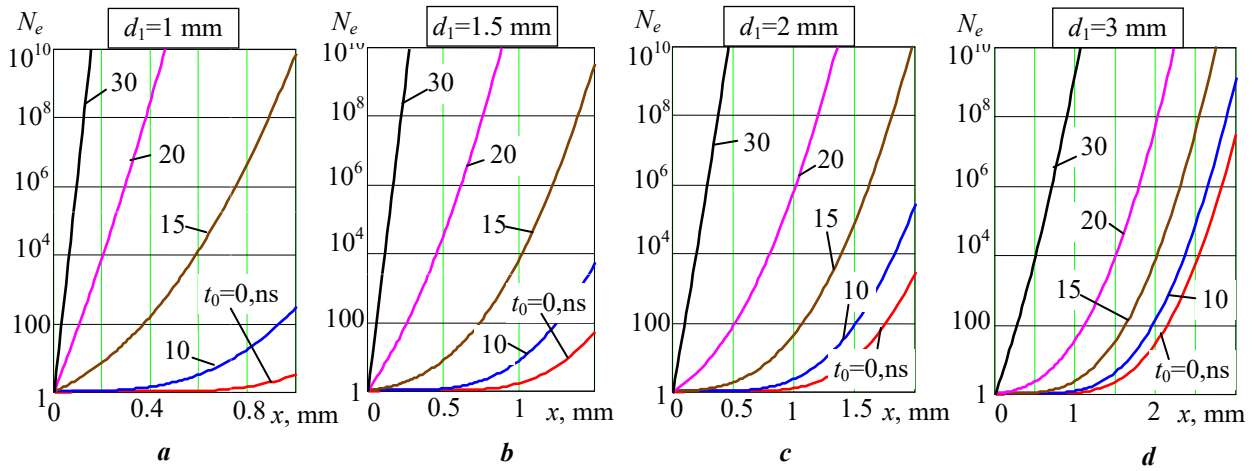


Fig. 7

Avalanche-streamer transition in the PDBD device. The study of the avalanche-streamer transition will be based on achieving condition (7), when the maximum value of the electric field strength of the space charge of the electron avalanche reaches the external field strength. The field strength of the space charge eN_e , in addition to the total charge value, depends on the geometry of the area of the space charge location, its size, and the charge distribution in the area. These characteristics are influenced by two main physical processes: diffusion extension of electron formation and electrostatic repulsion of electrons in the avalanche [10, 12, 16]. At the initial time point, the rate of growth of the avalanche size due to diffusion significantly exceeds the rate of its growth under the action of electrostatic repulsion. With the increase in the number of electrons in the avalanche, the rate of electrostatic repulsion increases sharply. In a constant field, starting from $N_e \sim 10^6$, the size of electron cloud is already determined by electrostatic repulsion [10, 12]. But in a rapidly growing pulsed field, when a significant overvoltage occurs, this relationship may change [12]. Therefore, it is necessary to consider these processes in more detail, taking into account the characteristics of the electric field pulse in the barrier discharge device.

When electrons drift with a velocity $v_{ed} = \mu_e E$, the electron cloud expands due to diffusion around the central point of the avalanche, the position of which is determined from (13). The electron flux density \mathbf{F} , taking into account the drift in the electric field and diffusion in vector form, is

$$\mathbf{F} = -n_e \mu_e \mathbf{E} - D_e \nabla n_e, \quad (15)$$

where n_e is the electron density, ∇ is the Hamilton differential operator.

Taking into account the rate of increase in electron density due to ionization $q = \alpha v_{ed} n_e$, the continuity equation for particles has the form [10]

$$\frac{\partial n_e}{\partial t} + \operatorname{div} \mathbf{F} = q. \quad (16)$$

The solution of equation (16) was obtained in [16] for avalanche originating from a single initial electron in the case of constant uniform external electric field. The electron density in the avalanche as a function of time $t_c = t - t_0$, the coordinate of the point $x - x_0$ and the distance r relative to the axial line of the avalanche movement is determined from the expression

$$n_e = (4\pi D_e t_c)^{-3/2} \exp \left[\alpha v_{ed} t_c - \frac{((x - x_0) - v_{ed} t_c)^2 + r^2}{4D_e t_c} \right]. \quad (17)$$

We will use (17) also for the pulsed field in the case when the avalanche is initiated at a time for which the electric field strength significantly exceeds the threshold value $\sim 30 \cdot 10^5$ V/m. Then, during a short period of time required to achieve condition (7) of transition the avalanche into the streamer, the external field strength changes by a small amount and, accordingly, the parameters in (17), determining the diffusion expansion of the electron cloud, change insignificantly.

To study the electric field strength of volume charge, the main issue is to obtain the dimensions of the area where the charge is concentrated, and its distribution in this area. To do this, at a certain moment of time from the beginning of the avalanche movement, we fix the central point of the avalanche $(x_c - x_0)$, which meets the condition $(x_c - x_0) - v_{ed} t_c = 0$. In this case, the expression (17) can be represented in the following form

$$n_e = (4\pi D_e t_c)^{-3/2} \exp \left[\alpha v_{ed} t_c - \frac{r^2}{4D_e t_c} \right] = (4\pi D_e t_c)^{-3/2} N_e(t_c) \exp \left(-\frac{r^2}{4D_e t_c} \right). \quad (18)$$

The distribution of electrons in moving avalanche has radial symmetry and its density decreases with distance from the center. The differential radius of the avalanche, at which the density decreases by a factor of e compared to its value at the center, is determined by the law $R_D = \sqrt{4D_e t_c}$. This value is often used to study the distortion of the electric field by the distributed charge and the achievement of condition (7) of the avalanche-streamer transition at this radius. The radius R_D differs from the radius at which the field strength reaches its maximum value R_m , which more closely corresponds to the content of condition (7).

The electric field strength of the charge distributed with the volume density en_e is determined by the expression

$$E'(r, t_c) = \frac{1}{4\pi\epsilon_0 r^2} \int_0^r en_e 4\pi r'^2 dr' = \frac{eN_e(t_c)}{\epsilon_0 (4\pi D_e t_c)^{-3/2}} f(r, t_c), \quad (19)$$

where only the function $f(r, t_c)$ depends on the radius r

$$f(r, t_c) = \frac{1}{r^2} \int_0^r r'^2 \exp \left(-\frac{r'^2}{4D_e t_c} \right) dr'. \quad (20)$$

The function $f(r, t_c)$ depends on the time t_c that has passed from the initiation of the avalanche t_0 to the current moment t . The diffusion coefficient D_e also depends on the electric field strength $E_0(t_c + t_0)$. The maximum of the function $f(r, t_c)$ gives the maximum electric field strength on the surface of a sphere of radius R_m for radially distributed charge. However, it should be noted that the difference between the radii R_D and R_m is not too large to significantly affect the results. For example, for

$d_1 = 2 \text{ mm}$, $t_0 = 23.7 \text{ ns}$, $t_c = 4 \text{ ns}$ we have the following values: $R_D = 5.1 \cdot 10^{-2} \text{ mm}$, $R_m = 4.75 \cdot 10^{-2} \text{ mm}$. In the future, to study the condition for achieving the avalanche-streamer transition (7), we will perform the calculations for the radius R_m .

Another reason for the growth of the head size of electron avalanche is electrostatic repulsion. It is usually assumed that it has a spherical shape [10, 12, 13]. The growth rate of the radius of the sphere is determined by the drift of electrons in the charge field of the avalanche. The assumption is valid when the external field does not affect the electron drift. This is explained by the superposition of fields - along direction of avalanche movement the field increases and, accordingly, the speed of the electrons increases too, in the opposite direction the field and the speed of the electron drift decrease. Only in the transverse direction the electric field strength is determined by charge of the electrons, however, to explain the basic properties of the process, the above assumption is usually made regarding the growth rate of the charged sphere

$$\frac{dR_F}{dt} = \mu_e E' = \mu_e \frac{eN_e}{4\pi\epsilon_0 R_F^2}. \quad (21)$$

The solution of equation (21) with respect to the radius of the sphere R_F is

$$R_F(t_c) = \left[\frac{3e}{4\pi\epsilon_0} \int_0^{t_c} \mu_e N_e dt \right]^{1/3}. \quad (22)$$

The maximum electric field strength E' of the distributed charge will be on the surface of the sphere radius R_F , the value of which is due to the electrostatic repulsion of electrons in the avalanche.

The growth of the avalanche radius due to electrostatic repulsion is limited by the braking effect associated with the opposing action of positive charges that are exposed when electrons leave them. It is believed that the size of the electron cloud is limited by the approximate condition when the radius is equal to the ionization length $R_F \sim \alpha^{-1}$.

Which of the mechanisms - diffusion or electrostatic repulsion - is predominant when the field strength of the distributed charge reaches the limiting value (7) depends on the rate of increase in the external electric field strength. As can be seen from Fig. 7, initially after applying voltage the number of electrons in the avalanches during the drift time to the anode does not reach the values typical for the avalanche-streamer transition. Therefore, let us consider the growth of the size of the electron avalanches, starting conditionally from the second and subsequent stages (second and subsequent generations). For the beginning of each subsequent stage, we will take the time moments t_0 corresponding to the drift time of electrons from the dielectric barrier to the anode during the previous stage. Such a choice for $d_1 = 1 \text{ mm}$ is to some extent justified by the fact that the largest number of electrons in the avalanche will be when it passes the maximum distance. According to the estimates of the number of electrons in the avalanche from Fig. 6 and 7, the avalanche-streamer transition can take place for the second generation near the anode. The choice for $d_1 = 3 \text{ mm}$ the beginning of the third generation is conditional, since already at the second stage the avalanche-streamer transition is realized when the avalanche reaches the middle area of the gap. Therefore, the choice t_0 at these stages does not characterize the development of the avalanche process, but only gives a discrete choice t_0 .

Fig. 8 shows the dynamics of the growth of the electron cloud radius. The calculation results are shown for two extreme cases of the air gap $d_1 = 1 \text{ mm}$ and $d_1 = 3 \text{ mm}$. Fig. 8, *a* and Fig. 8, *c* refer to the gap $d_1 = 1 \text{ mm}$, Fig. 8, *b* and Fig. 8, *d* refer to $d_1 = 3 \text{ mm}$. In the figures for the same d_1 the data differ by the beginning moment t_0 of the avalanches development for the second and third avalanche generations. The maximum value of the selected time intervals of the growth of the radius of avalanches approximately corresponds to the time of reaching the critical number of electrons in the avalanche, when it transforms into the streamer form.

The presented dependences show an initially slow, and over time a very rapid growth of the avalanche radius due to electrostatic repulsion, the speed of which begins to significantly exceed the diffusion growth. At the same time, the radius limitation $R_F \leq \alpha^{-1}$ shows that for the pulsed process the diffusion

radius exceeds the radius of electrostatic repulsion. This radius ultimately determines the condition of achievement of the avalanche-streamer transition. This situation occurs both at the second and third stages of avalanche development.

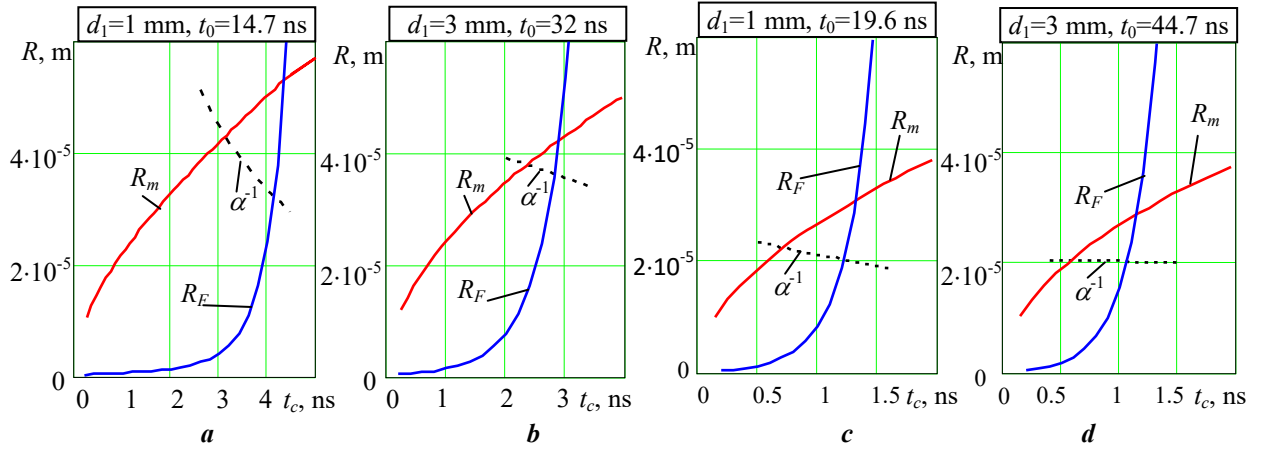


Рис. 8

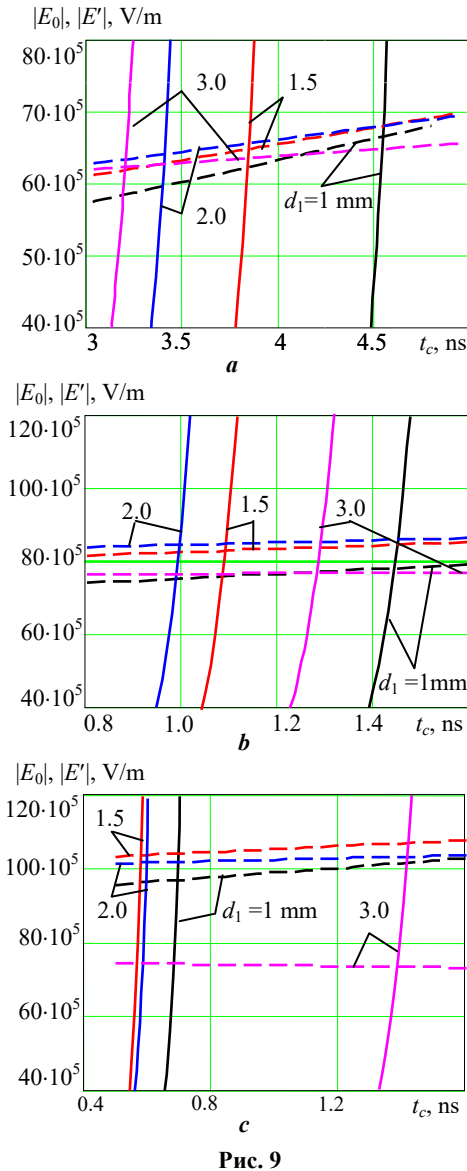


Рис. 9

If the process continues further, then due to the increase in the field strength in subsequent generations, the diffusion radius, as before, will be decisive.

For different air gaps, we will determine the main parameters at which the avalanche transforms into the streamer. To do this, it is necessary to find a solution to equation (7), where the left part is determined from (19), and the right part is the given external electric field (1), (4) for the selected initial data: $U_m = -25 \cdot 10^3$ V, $n = 2$, $\omega = \pi \cdot 10^7$ s⁻¹. The equation was solved relative to the time $t_c = t_s$ of occurrence of the condition of the avalanche-streamer transition at the given values of the air gap d_1 and the time t_0 of the beginning of the avalanche development. For each d_1 the three consecutive values of time t_0 were conditionally selected, which, as before, are counted from the start of the applied voltage to the time that would be required for the electron to overcome one, double and triple distances d_1 .

Fig. 9 for each d_1 illustrates the change in time of the external field strength $|E_0|$ (dashed line) and the field strength of the electron avalanche charge $|E'|$ (solid curves) near the fulfillment of condition (7) for the three specified time points t_0 . The intersection of the corresponding curves gives the time of the avalanche transition into the streamer and the electric field strength of the such transition. In addition to these data, Table 2 also shows other transition parameters: the distance that moved the avalanche $x_s - x_0$, the number of electrons in the avalanche at the moment of transition N_{es} , radius of the avalanche R_{ms} , the average energy of electrons, which is related to their temperature in the avalanche $\bar{W}_{es} = \frac{3}{2} kT_{es}$. The data for three consecutive time points t_0 , to which Fig. 9, a, b, c correspond, are located one below the other in the Table 2.

For the second generation of electron avalanches (Fig. 9, *a*),

Table 2							
d_1 , m	t_0 , ns	t_s , ns	$x_s - x_0$, m	N_{es}	R_{ms} , m	E_s , V/m	\overline{W}_{es} , eV
$1 \cdot 10^{-3}$	14.67	4.54	$0.90 \cdot 10^{-3}$	$3.43 \cdot 10^7$	$5.45 \cdot 10^{-5}$	$66.5 \cdot 10^5$	7.51
	19.63	1.44	$0.37 \cdot 10^{-3}$	$1.44 \cdot 10^7$	$3.24 \cdot 10^{-5}$	$78.0 \cdot 10^5$	8.74
	23.35	0.69	$0.20 \cdot 10^{-3}$	$0.95 \cdot 10^7$	$2.38 \cdot 10^{-5}$	$97.0 \cdot 10^5$	10.2
$1.5 \cdot 10^{-3}$	19.35	3.84	$0.79 \cdot 10^{-3}$	$2.80 \cdot 10^7$	$4.96 \cdot 10^{-5}$	$64.8 \cdot 10^5$	7.31
	26.04	1.09	$0.29 \cdot 10^{-3}$	$1.18 \cdot 10^7$	$2.87 \cdot 10^{-5}$	$82.8 \cdot 10^5$	9.19
	31.30	0.58	$0.18 \cdot 10^{-3}$	$0.89 \cdot 10^7$	$2.21 \cdot 10^{-5}$	$103.7 \cdot 10^5$	10.5
$2 \cdot 10^{-3}$	23.72	3.41	$0.72 \cdot 10^{-3}$	$2.41 \cdot 10^7$	$4.65 \cdot 10^{-5}$	$64.1 \cdot 10^5$	7.22
	32.20	1.0	$0.27 \cdot 10^{-3}$	$1.11 \cdot 10^7$	$2.75 \cdot 10^{-5}$	$84.4 \cdot 10^5$	9.33
	39.13	0.60	$0.18 \cdot 10^{-3}$	$0.88 \cdot 10^7$	$2.23 \cdot 10^{-5}$	$101.7 \cdot 10^5$	10.4
$3 \cdot 10^{-3}$	32.04	3.20	$0.69 \cdot 10^{-3}$	$2.14 \cdot 10^7$	$4.46 \cdot 10^{-5}$	$62.3 \cdot 10^5$	7.02
	44.70	1.28	$0.33 \cdot 10^{-3}$	$1.22 \cdot 10^7$	$3.03 \cdot 10^{-5}$	$76.6 \cdot 10^5$	8.60
	56.15	1.39	$0.35 \cdot 10^{-3}$	$1.23 \cdot 10^7$	$3.11 \cdot 10^{-5}$	$73.6 \cdot 10^5$	8.29

for all gaps d_1 , the characteristic field strength of the avalanche-streamer transition is $E_s \sim 60 \cdot 10^5$ V/m. In this case, the avalanche development time is within $t_s \approx 3 - 4.5$ ns, increasing with decreasing gap d_1 . The distance that the avalanche moves before its transformation is different for different gaps. At the smallest $d_1 = 1$ mm, the transformation of the avalanche into streamer takes place near the anode, when the avalanche has overcome almost the entire gap. That is, the electrons that appear directly at the dielectric barrier will be effective in generating streamers. For larger gaps, electrons appearing in a wider part of the air gap will be effective. This applies to relatively large gaps to the greatest extent.

For example, for $d_1 = 3$ mm, the avalanche only needs to move the distance $x_s - x_0 = 0.69$ mm, i.e., initial electrons appearing at almost any point in the gap will be effective. Moreover, each avalanche, and especially the avalanche that has turned into the streamer, is an intense source of photons. Therefore, photo-ionization in this case is generated by avalanches that appeared not only at the time t_0 of the beginning of the second stage. During the time between the beginning of the second and the next stages, several successive avalanche processes are generated. They also generate photons. The average energy of electrons in the avalanche, which turns into streamer, at this stage depends only slightly on the size of the discharge gap and is $\overline{W}_{es} \approx 7 - 7.5$ eV. The average energy of electrons in the avalanche and the corresponding electron temperature are determined from (8) for the electric field strength E_s . Since such field strength is realized in certain areas of the avalanche and the issue of energy relaxation in the field that changes rapidly in time and space has not been investigated, the given value of the average energy of electrons under conditions of thermodynamic equilibrium gives only estimated values.

For the following selected values of time t_0 from the beginning of the voltage pulse, all the above-mentioned features occur, which, however, are much more intense. So, for the next time stage after considered (the third stage of avalanche generations, Fig. 9, *b*, the second row in the Table 2), the electric field strength of the avalanche-streamer transition has the larger value $E_s \sim 80 \cdot 10^5$ V/m, the time of avalanche development decreases to values $t_s \approx 1 - 1.5$ ns, the growing avalanches cover shorter distance $x_s - x_0 \sim 0.3 - 0.4$ mm and, accordingly, several successive systems of avalanches and streamers may appear until next time t_0 . In the electric field of greater intensity, the average energy of electrons at the moment of its transition into the streamer also increases $\overline{W}_{es} \approx 8.6 - 9.3$ eV, and larger values are achieved for the average value of the gap $d_1 = 1.5$ mm and $d_1 = 2$ mm.

Even more extreme parameters occur with a further increase in the pulse voltage, which is reflected in Fig. 9, *c* and in the third row of the Table 2 elements. Here, the electric field strength of the transition of avalanches to the streamer form has values $E_s \sim 100 \cdot 10^5$ V/m (except for the case $d_1 = 3$ mm where the field strength in the gap is the smallest and already decreases at given time interval). The distance that avalanches need to move before the transition has even smaller values $x_s - x_0 \sim 0.2$ mm and in essence it is nec-

essary to consider a continuous process of avalanche-streamer transitions. The number of streamers in the gap increases even more. The average energy of electrons in the avalanche for the gaps $d_1 = 1 - 2$ mm also increases slightly $\overline{W}_{es} \approx 10.2 - 10.5$ eV, almost not differ for different gaps.

Referring to Fig. 2, *a* of the experimentally measured time dependences of the pulse voltage and current for the gap $d_1 = 1.5$ mm, we can make an assumption about the explanation of the current reaching its maximum at $E_0 \approx 90 \cdot 10^5$ V/m through ~ 30 ns after the beginning of the voltage pulse increase. These measured parameters are consistent with the calculated ones for three or four stages of the avalanche process development.

The explanation may lie in the strong increase in the number of electron avalanches that transform into streamers with increasing pulsed electric field strength. At this, the time required for avalanches to transform into streamer form is significantly reduced. In addition to the significant drift velocity of avalanches, each streamer, growing in both directions towards the anode and the cathode, almost short-circuits the gap [10], leaving a positive charge on the dielectric barrier. In the place where the streamer touches the barrier, the entire voltage is applied to the dielectric plate. In order for the average value of the electric field strength throughout the air gap reaches the required minimum, which corresponds to a significant reduction or termination of ionization processes, the surface density of the positive electric charge on the dielectric barrier must have a certain minimum value. Such a value probably determines at the same time the average distance between the streamers that have reached the barrier. In such process, after very rapid transfer of charges over time ≤ 1 ns and, accordingly, a significant current, the movement of charges will stop. After that, as can be seen from Fig. 2, the current in the outer circuit decreases sharply and is determined mainly insignificant (by the estimated) capacitive current through the dielectric barrier.

If the voltage continues to increase, the field strength in the gap increases again. This can lead to the appearance of another local extremum for the current, which is often observed in experiments. The extremum is clearly visible in the graph of Fig. 2, *b* and is noticeable near the zero current value in Fig. 2, *a*. After a second surge, the current reaches zero value at the moment of the voltage maximum, which is characteristic of the capacitive current. Regarding the second local current extremum, it should be noted that its appearance may also be due to another reason. In [18], the appearance of the extremum was explained by the arrival of a reflected current wave propagating along a high-voltage cable. The real reason for the appearance of the second extremum in the current oscillogram requires additional investigation.

The assumptions given above define only one of the necessary directions for further research. However, it seems that in the study of electrical discharge processes, and especially pulsed ones with the presence of the dielectric barrier, the determining factor remains the experiment, the correspondence to the results of which is mandatory in theoretical research.

Conclusions.

1. Computational studies of the avalanche stage of the pulsed barrier discharge with the dielectric barrier located on the cathode, which were carried out for the specific electrode system with air gaps within $1 \div 3$ mm, voltage pulse with the amplitude of 25 kV and time of its achievement 50 ns, showed that the condition of the avalanche-streamer transition is achieved during the growth of avalanches starting at photoionization by photons that appear as a result of impact ionization in the gas and take place from the second stage of avalanche generation. After three or four stages, the avalanche-streamer transition occurs at the voltage that slightly depends on the air gap and has value in the range of 80-100 kV/cm. For the test gap of 1.5 mm, this value, as well as the time ~ 30 ns after voltage application when this field strength is reached, is consistent with the same value in the experiment at the moment when the maximum current value is reached.

2. For the considered air gaps and pulse voltage parameters in the pulsed barrier discharge device, the radius of the electron avalanche, which together with the number of electrons gives the electric field strength of the avalanche-streamer transition, is determined by electron diffusion and exceeds the size of the avalanche, which expands due to the phenomenon of electrostatic repulsion.

3. At the first stage of electron drift, which starts with the beginning of the voltage pulse and ends when the electrons reach the anode the number of ionizations capable of emitting the required number of photons strongly depends on the size of the air gap in the range under consideration: for gap smaller than 1.5 mm, due to the small number of ionizations in the avalanche, the probability of photon emission is small and after the end of this stage the gap remains without of the initial electrons; for air gaps greater than 1.5 mm, as a result of the first stage of the avalanche movement, the conditions of the multi-channel avalanche

process are met due to photo-ionization; a gap of ~1.5 mm seems to be transitional from the point of view of the continued development of the pulsed barrier discharge due to photo-ionization at the first stage.

The work was supported by state project "Development of the theory and modeling of non-stationary electrophysical processes in the conducting and dielectric media of the pulsed electromagnetic systems" ("Barrier-3"), KPKVK 6541030.

1. Xin Pei Lu, Mounir Laroussi. Temporal and spatial emission behavior of homogeneous dielectric barrier discharge driven by unipolar sub-microsecond square pulses. *Journal of Physics D: Applied Physics*. 2006. Vol. 39. Pp. 1127-1131. DOI: <https://doi.org/10.1088/0022-3727/39/6/018>.
2. Shao Tao, Long Kaihua, Zhang Cheng, Yan Ping, Zhang Shichang, Pan Ruzheng. Experimental study on repetitive unipolar nanosecond-pulse dielectric barrier discharge in air at atmospheric pressure. *Journal of Physics D: Applied Physics*. 2008. Vol. 41. 215203 (8pp). DOI: <https://doi.org/10.1088/0022-3727/41/21/215203>.
3. Shuai Zhang, Li Jia, Wen-chun Wang, De-zheng Yang, Kai Tang, Zhi-jie Liu. The influencing factors of nanosecond pulse homogeneous dielectric barrier discharge in air. *Spectrochimica Acta Part A: Molecular and Biomolecular Spectroscopy*. 2014. Vol. 117. Pp. 535-540. DOI: <https://doi.org/10.1016/j.saa.2013.08.051>.
4. Kogelschatz U. Review Dielectric-barrier Discharges: Their History, Discharge Physics, and Industrial Applications. *Plasma Chemistry and Plasma Processing*. 2003. Vol. 23. No 1. Pp. 1-47. DOI: <https://doi.org/10.1023/A:1022470901385>.
5. Schmidt M., Holub M., Jogi I., Sikk M. Treatment of industrial exhaust gases by a dielectric barrier discharge. *Eur. Phys. J. Appl. Phys.* 2016. No 75. P. 24708. DOI: <https://doi.org/10.1051/epjap/2016150554>.
6. Bozhko I.V., Bereka V.O. Uniform of pulse barrier discharge in the air of atmospheric pressure in the presence of water in a drop-film condition. *Tekhnichna Elektrodynamika*. 2019. No 5. Pp. 17-21. DOI: <https://doi.org/10.15407/technd2019.05.017>. (Ukr)
7. Bereka V.O., Bozhko I.V., Kondratenko I.P. Influence of parameters of water movement at its treatments on energy efficiency pulse barrier discharge. *Tekhnichna Elektrodynamika*. 2022. No 3. Pp. 62-68. DOI: <https://doi.org/10.15407/technd2022.03.062>. (Ukr)
8. Lobanov L.M., Berdnikova O.M., Pashchyn M.O., Mykhoduj O.L., Kushnaryova O.S., Solomiychuk T.G., Kryvyi V.I. Strengthening of welded structures of 25KHGNMT steel by pulsed barrier discharge treatment. *Avtomaticheskaya Svarka (Automatic Welding)*. 2022. No 12. Pp. 3-8. DOI: <https://doi.org/10.37434/as2022.12.01>. (Ukr)
9. Bozhko I.V., Kondratenko I.P., Lobanov L.M., Pashchin M.O., Berdnikova O.M., Mykhodui O.L., Kushnarova O.S., Goncharov P.V. Pulsed barrier discharge for treatment of surfaces of 25XHTMT steel plates. *Tekhnichna Elektrodynamika*. 2023. No 1. Pp. 76-81. DOI: <https://doi.org/10.15407/technd2023.01.076>. (Ukr)
10. Rizer Yu.P. Gas Discharge Physics. Springer. Berlin Heidelberg, 2011. 449 p. (Rus).
11. Meek J.M., Craggs J.D. Electrical Breakdown of Gases. Wiley, 1953. 507 p. DOI: <https://doi.org/10.1002/qj.49708034425>.
12. Korolev Yu. D., Mesyats G. A. Physics of Pulsed Breakdown in Gases. Ural Division of the Russian Academy of Sciences, 1998. 274 p. (Rus)
13. Beyer M., Boeck W., Möller K., Zaengl W. Hochspannungstechnik. Theoretische und praktische Grundlagen. Springer-Verlag Berlin Heidelberg, 1986. XIII, 362 p. DOI: <https://doi.org/10.1007/978-3-642-61633-4>.
14. Granovsky V. L. Electric Current in a Gas. Steady-State Current. Moskva: Nauka, 1971. 543 p. (Rus)
15. Raether H. Electron Avalanches and Breakdown in Gases. London: Butterworths, 1964. 191 p.
16. Lozansky E.D. and Firsov O.B. The Theory of the Spark. Moskva: Atomizdat, 1975. 272 p. (Rus).
17. Bereka V.O., Bozhko I.V., Karlov O.M., Kondratenko I.P. Coordination of parameters of the power source and the working chamber for water treatment with pulse barrier discharge. *Tekhnichna Elektrodynamika*. 2023. No 4. Pp. 81-89. DOI: <https://doi.org/10.15407/technd2023.04.081>. (Ukr).
18. Bereka V.O., Vasetsky Yu.M., Kondratenko I.P. The influence of the connecting high-voltage cable to the currents and voltages in device of pulsed dielectric barrier discharge. *Tekhnichna Elektrodynamika*. 2023. No 4. Pp. 81-89. DOI: <https://doi.org/10.15407/technd2024.04.016>. (Ukr).
19. Atomic and Molecular Processes. Editor: D.R. Bates. Academic Press, 1962. 904 p.
20. Razevig D.V. High Voltage Engineering. Khanna Publishers, 2011. 726 p.
21. Teich T.H. Emission gasionisierender Strahlung aus Elektronenlawinen. I. Meßanordnung und Meßverfahren. Messungen in Sauerstoff. *Zeitschrift Fur Physik*. 1967. Bd 199. H. 4. Pp. 378-394. DOI: <https://doi.org/10.1007/bf01332287>.
22. Teich T.H. Emission gasionisierender Strahlung aus Elektronenlawinen. II. Messungen in Oz-He-Gemischen, D-impfen, CO₂ und Luft; Datenzusammenstellung. *Zeitschrift Fur Physik*. 1967. Bd 199. H. 4. Pp. 395-410. DOI: <https://doi.org/10.1007/BF01332288>.

ЕЛЕКТРОФІЗИЧНІ ПРОЦЕСИ РОЗВИТКУ ЛАВИН ЕЛЕКТРОНІВ В ПОВІТРІ У ПРИСТРОЇ ІМПУЛЬСНОГО ДІЕЛЕКТРИЧНОГО БАР'ЄРНОГО РОЗРЯДУ

Ю.М. Васецький, докт. техн. наук
Інститут електродинаміки НАН України,
пр. Берестейський, 56, Київ, 03057, Україна.
E-mail: yuriv.vasetsky@gmail.com.

Метою роботи є визначення впливу величини міжелектродного проміжку і часової залежності зростання імпульсного електричного поля на характеристики лавинної стації імпульсного бар'єрного розряду від початку дрейфу електронів у поступово зростаючому електричному полі з урахуванням порогового характеру процесу ударної іонізації в газі, впливу фотоіонізації на розмноження лавин, дифузії і електростатичного розштовхування електронів до моменту досягнення у головці лавини умови початку стрімерного процесу. Розрахункові дослідження проведені для конкретної електродної системи з діелектричним бар'єром на катоді для газового проміжку 1–3 мм, імпульсу напруги з амплітудою 25 кВ і часом її досягнення 50 нс. Знайдено, що після трьох-чотирьох етапів генерації лавин їх перетворення у стрімері відбувається за напруженості поля 80-100 кВ/см, який настає через ~30 нс після подачі напруги і слабо залежить від величини газового проміжку. З'ясовано, що для експерименту з тестовим проміжком 1.5 мм такі значення напруженості і часу мають місце в момент досягнення максимальної величини струму. Встановлено, що розміри лавини електронів для заданого імпульсу напруги у пристрої імпульсного бар'єрного розряду визначаються процесом дифузії електронів. Показано, що після подачі напруги в результаті першого етапу дрейфу електронів кількість випромінених фотонів, здатних породжувати ефективні електрони для подальшого розвитку лавинного процесу, сильно залежить від величини розрядного проміжку. Визначено межі довжин проміжків із суттєво різною можливістю ініціювати розвиток лавин на наступних етапах. Бібл. 22, рис. 9, табл. 2.

Ключові слова: імпульсний діелектричний бар'єрний розряд, лавинно-стрімерний перехід, фотоіонізація, напруженість електричного поля лавини електронів.

Received 10.12.2024

Accepted 19.12.2024